Progress In Electromagnetics Research M, Vol. 39, 65–75, 2014

Triple Band Circular Ring-Shaped Metamaterial Absorber for X-Band Applications

Osman Ayop, Mohamad K. A. Rahim*, Noor A. Murad, Noor A. Samsuri, and Raimi Dewan

Abstract—This paper presents the design, fabrication, and measurement of triple band metamaterial absorber at 8 GHz, 10 GHz and 12 GHz which are in the X-band frequency range. The unit cell of the metamaterial consists of three concentric copper rings at different radii, printed on 0.8 mm thick FR4 substrate in order to obtain triple resonant frequencies. The highly symmetrical ring structure in nature makes this absorber insensitive to any polarization state of incident electromagnetic (EM) waves for normal incident waves. The proposed structure is capable to operate at wide variations angle of incident wave. The simulated result shows that the triple-band metamaterial absorber achieves high absorbance for normal incident electromagnetic waves of 97.33%, 91.84% and 90.08% at 8 GHz, 10 GHz and 12 GHz, respectively, when subjected to normal incident electromagnetic. With metamaterial absorber maintaining 50% of absorbance value, the corresponding full width half maximum (FWHM) are 5.61%, 2.90% and 2.33%. The operating angles in which the metamaterial structure can maintain 50% absorbance at TE mode and TM mode are 67° and 64°, respectively. The experimental result verifies that the absorber is well performed at three different resonant frequencies with absorbance greater than 80%.

1. INTRODUCTION

Metamaterials have attracted many researchers for many years due to their unique properties which can be integrated to several devices to improve the desired performance. Metamaterial structures are artificially engineered structures with unique electromagnetic properties that are not found in nature [1]. The structures are typically developed by periodic arrangement of metallic unit cell on dielectric layer. Some metamaterials are designed in aperiodic form [2], and some are designed by having multiple layers with same materials [3] or different materials [4]. An example of metamaterial is left-handed metamaterial which was designed using the principle of double negative permeability, μ, and permittivity, ε, [5–7]. Left-handed metamaterial does not exist in nature but can be artificially realized. However, simultaneous negative value of μ and ε can be achieved in certain range of frequencies [8]. Most researches have taken into account the aspects of real part of μ and ε in their design of metamaterial. By considering the imaginary part which also contributes to the loss, the metamaterial electromagnetic absorber can be constructed. The development of metamaterial as absorbers potentially creates electromagnetic devices with amazing performance over a wide range of operating frequency. The applications of the metamaterial include the invisibility cloaks, bolometer, spectroscopy, thermal emission and sub-wavelength imaging [9–13].

EM based metamaterial absorbers are designed based on the principle of lossy surface which matches with the free space impedance at resonant frequency [14]. To fulfill this condition, the imaginary part of refractive index, $n(\omega)$, which contributes to the energy loss, should be large enough. This can be

Received 24 May 2014, Accepted 1 September 2014, Scheduled 6 October 2014

* Corresponding author: Mohamad Kamal Abd Rahim (mkamal@fke.utm.my).
The authors are with the Department of Communication Engineering (COMM), Faculty of Electrical Engineering, Universiti Teknologi Malaysia (UTM), Johor Bahru 81310, Malaysia.

achieved by proper design of the metamaterial structure [15, 16]. Simultaneously, the values of $\mu(\omega)$ and $\varepsilon(\omega)$ should be the same in order to achieve the condition where metamaterial absorber impedance is $Z(\omega) = 1$ which indicates that the impedance of the structure matches the free space impedance [17].

Perfect metamaterial absorbers are achieved if both transmission and reflection of incidental waves are zero. Hence, the maximum absorbance of the metamaterial absorber is obtained. However, this condition occurs only in narrow frequency range for most metamaterial absorber designs. Many works have been done to enhance the operating frequency of the metamaterial absorber such as designing them in multi-band and broader bandwidth [18, 19]. Such designs are quite challenging because they require perfect impedance that match the free space to obtain large losses. Apart from absorbance issue, the metamaterial absorber should be polarization insensitive which will not limit the desired application. The polarization sensitive types of absorber can work for EM waves with one particular polarization only. Additionally, good metamaterial absorber should be capable to operate at large variation angle of incident EM wave.

In 2008, Landy et al. [20] demonstrated the first experimental result of metamaterial specifically characterized as an electromagnetic (EM) absorber. The nearly perfect absorber was designed using Electric Field Driven LC (ELC) resonator on cut-wire separated by a dielectric layer. However, this structure only works on single frequency, polarization dependent and had large thickness. Since then, number of simulation and experimental results are published related to metamaterial-based EM absorber from radio up to the optical frequency [21–23]. Another ELC based metamaterial absorber was proposed by Tao et al. [24] in the terahertz frequency band, which consists of two dielectric layers, an ELC and a metallic layer. This structure had a wide angular bandwidth, but it is still polarization sensitive with large thickness. Dincer et al. [25] proposed a design of metamaterial absorber which consists of an isotropic ring resonator with gaps, known as Octa-star strip (OSS) structure located at the top substrate, and a metallic layer located at the bottom substrate. Both layers are separated by a dielectric substrate. This structure is independent of polarization and incident angle variation which has a strong dual-band resonant. Sabah et al. [26] introduced a perfect frequency selective surface (FSS) metamaterial absorber (MAs) based on resonator with dielectric configuration in microwave and optical frequency ranges. Six different structures were examined which showed perfect absorption, polarization independent and incident angle independencies. The proposed structures were also simple and easy to tune at desired frequency. Huang and Chen [27] designed a metamaterial absorber based on rectangular ring structure. This structure operates at three different frequency bands which are C-, X-, and Ku-bands. The results show that the structure is polarization insensitive and operate at wide variation of incident angle. Sun et al. [28] proposed a metamaterial absorber design using multilayer slit ring resonator (SRRs) structure of an extremely broad frequency band absorber. The multilayer structure is used to induce a successive anti-reflection in wide frequency range. The drawback of this design is that it needs four layers, resulting in the increment of overall thickness.

In this paper, a triple-band circular ring metamaterial absorber is presented. The structure resonates at three different frequencies which are 8 GHz, 10 GHz and 12 GHz. Simulation and experimental procedures are conducted to determine the absorbance characteristics for variation of polarizations of normal incident EM waves. Next, the performance of the absorber for both transverse electric (TE) and transverse magnetic (TM) waves with oblique incident angle up to 60° is investigated in the experiment. EM field and current distributions are analyzed to demonstrate the physical behavior of the absorber. The advantages of the proposed structure are high symmetry, simple design, wide operating angle, thin substrate and multi-band operation with high absorbance. Due to the nature of circular ring shape which is highly symmetrical, it is not sensitive to any polarization states for normal incident waves. The design is also simple so that the dimension can be easily changed to operate at other frequencies. The designed absorber can also operate in wide angle of incident EM waves.

2. METAMATERIAL ABSORBER DESIGN AND SIMULATION

The design of triple-band circular ring metamaterial structure using FR4 material with dielectric constant of 4.6 and loss tangent of 0.019 is shown in Figure 1. The schematic of the proposed unit cell metamaterial structure consists of dielectric substrate sandwiched by two metallic layers. The top metallic layer is triple resonant copper layer constructed by three circular rings structure with different

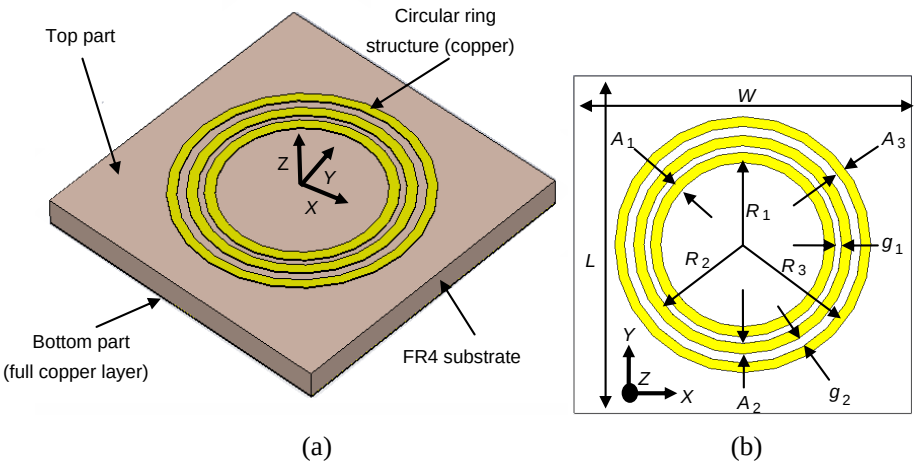

Figure 1. The geometry of the unit cell of triple band circular ring metamaterial absorber; (a) perspective view and (b) front view.

radii and widths. The rings are separated by two gaps of different sizes and optimized using full wave simulation. The bottom metallic layer is a full copper ground plane. The size of the substrate for the unit cell is 9 mm × 9 mm × 0.8 mm ($W \times L \times h$). The radii of the circular ring structures, R_1, R_2 and R_3, which contribute to the electrical resonance, are 2.33 mm, 2.78 mm and 3.29 mm, respectively. The widths of the rings, A_1, A_2 and A_3, are 0.28 mm, 0.28 mm and 0.26 mm, respectively. The gap between the rings, g_1 and g_2, are 0.24 mm and 0.17 mm, respectively. g_1 is the gap between the second largest ring and the smallest ring while g_2 is the gap between largest and the second largest rings.

The resonant frequency of the ring highly depends on the effective length of the ring and less dependent on the width of the ring. By selecting the reasonable widths of the rings, the absorbance value can be optimized. The gaps between rings are needed to separate ring structures to obtain different resonant frequencies. The gaps between the rings do not significantly influence the resonant frequencies but will influence the magnitudes of the metamaterial absorber. This is because the circular ring structure is an electric resonator. The existence of gaps acting as capacitors which coupled the electric component of incident electromagnetic waves. When the circular rings structure is strongly coupled to the incident electric field, it contributes to the frequency dependent electric response. However, it has a weak response to the incident magnetic field. To improve the design further, a full metallic ground layer is placed at the bottom of the substrate to improve the magnetic coupling due to the magnetic field incident waves. The flux of the incident magnetic component can be coupled within the dielectric layer and produces anti-parallel surface current due to the existence of a full copper ground layer at the bottom substrate. The advantage of using full metallic ground layer is that the analysis can be simplified by minimizing the value of reflectance. To obtain the maximum absorbance, the transmittance value is zero for all frequency ranges.

The simulation is carried out with advanced EM simulator (CST software) using frequency solver. The S-parameter results are obtained from the simulation and analyzed. The absorbance, $A(\omega)$, can be calculated by $A(\omega) = 1 - |S_{11}|^2 - |S_{21}|^2$. Since the full metal layer is used in this design, S_{21} is zero for all cases. Therefore, the analysis can be simplified to $A(\omega) = 1 - |S_{11}|^2$. The simulation result of the normal incident waves for triple band circular ring metamaterial absorber is presented in Figure 2. The result shows high absorbance at all three resonance frequencies which are 97.33%, 91.84% and 90.08% at 8 GHz, 10 GHz and 12 GHz, respectively, with the corresponding FWHM of 5.51%, 3.42% and 2.65. The triple resonant frequency of 8 GHz, 10 GHz and 12 GHz is contributed by the largest, middle and smallest circular rings, respectively.

To understand the physical behavior of the metamaterial absorbers, the electric field distribution, magnetic field distribution and surface currents are simulated at all resonance frequencies. Figure 3 shows the electric field distribution for triple-circular-ring metamaterial absorber. It can be observed that for the case of E-field, the concentration of power loss distribution is strong at $+y$ and $-y$-axes

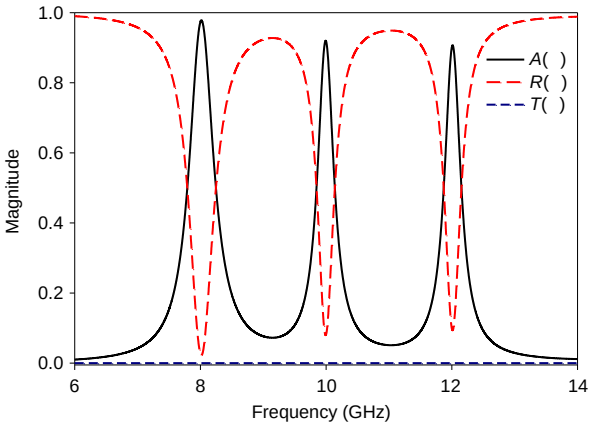

Figure 2. Reflectance, transmittance and absorbance of triple band circular ring metamaterial absorber.

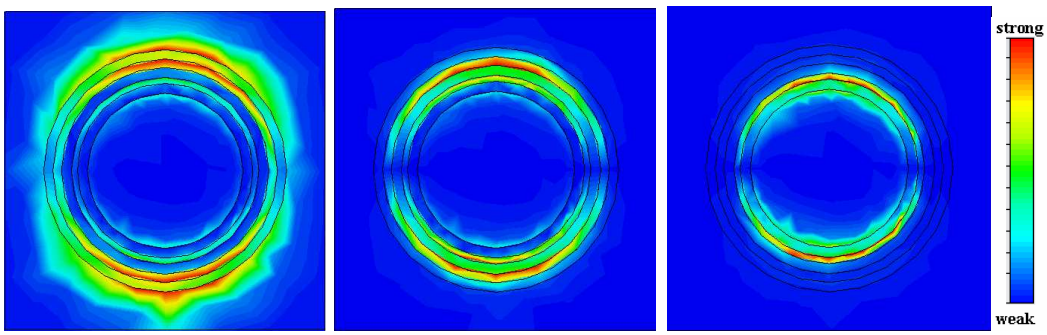

Figure 3. Electric field distribution for triple band circular ring metamaterial absorber at (a) 8 GHz, (b) 10 GHz, and (c) 12 GHz.

of the ring structure since it is parallel to the electric field component of the incident EM waves. At the first resonance frequency of 8 GHz, the concentration of E-field current is strong at g_2 as shown in Figure 3(a). This is because the first resonance is contributed by the largest circular ring so that the electric field component is coupled to the gap between the largest and the middle circular rings. Figure 3(b) shows the E-field distribution for the second resonance frequency at 10 GHz. From the figure, strong current is noticeable at g_1 and some significant amount of current distribution seen at g_2. The reason is that the middle circular ring provides the second resonance at 10 GHz so that the electrical component is coupled at both gaps of g_1 and g_2. For the third resonance frequency as shown in Figure 3(c), the electric field distribution is strong at g_2 due to the resonant element of the smallest circular ring. The electrical component of the third resonance is coupled to the g_2 between the smallest and middle circular rings.

For H-field, the concentration of power loss distribution is strong at $+x$ and $-x$-axes and weak at $-y$ and $+y$-axes of the ring. This is due to the magnetic component of EM waves, which is parallel to the x-axis of the ring structure. At the first resonance of 8 GHz, the concentration of the H-field current is strong at g_2 as shown in Figure 4(a). This is because the first resonance is contributed by the largest circular ring so that the magnetic field component is coupled to the gap between the largest and the middle circular rings. For the second resonance at 10 GHz, strong current is noticed at g_1, and some significant amount of current distribution is noticed at g_2 as shown in Figure 4(b). As mentioned previously, the middle circular ring provides the second resonance at 10 GHz so that the magnetic component is coupled at both gaps of g_1 and g_2. For the third resonance shown in Figure 4(c), the magnetic field distribution is strong at g_2 due to the resonant element of smallest circular ring. The

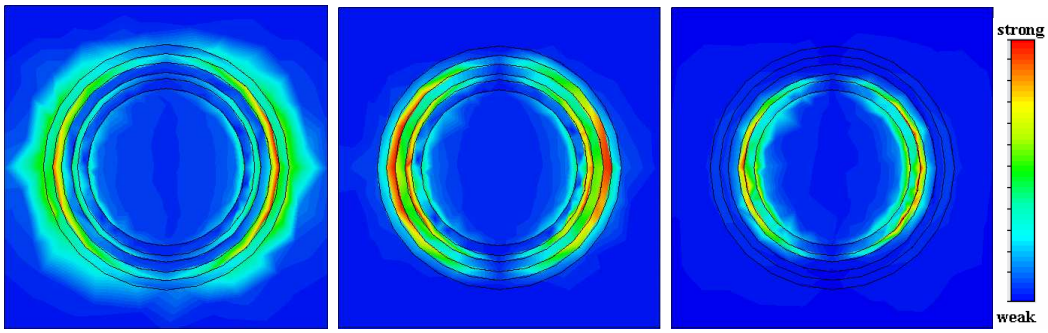

Figure 4. Magnetic field distribution for triple band circular ring metamaterial absorber at (a) 8 GHz, (b) 10 GHz, and (c) 12 GHz.

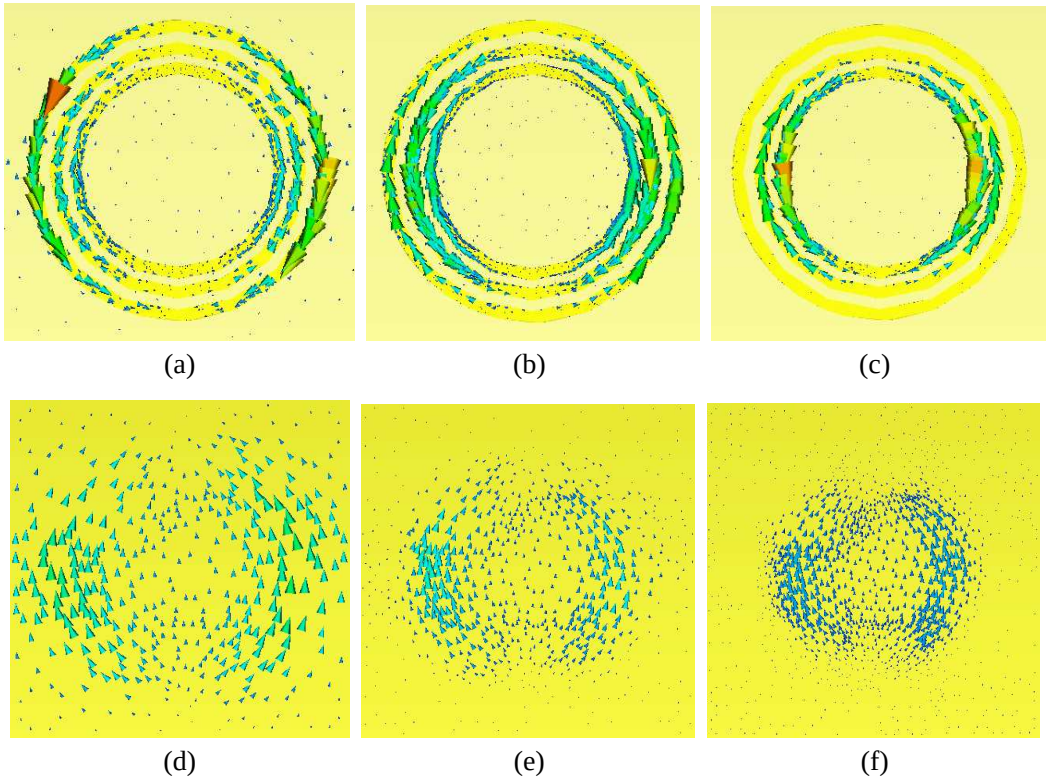

Figure 5. Surface current distribution for triple band circular ring metamaterial absorber at top layer: (a) 8 GHz, (b) 10 GHz, (c) 12 GHz and bottom metallic layer: (d) 8 GHz, (e) 10 GHz, (f) 12 GHz.

magnetic component of third resonant is coupled to g_2 between the smallest and middle circular rings. The simulated current distribution shows that the resonance characteristic between E- and H-fields is the same except for the location of the current distribution, which is perpendicular to each other.

Subsequently, the surface current distribution is investigated. Upon interaction with incident electromagnetic waves, the dipolar response is observed in which the currents flow upward and downward alternately at the left and right sides of the ring as shown in Figure 5. There are also magnetic responses associated with circulating displacement currents between the two metallic layers that contribute to the power loss in the metamaterial structure. The dipolar pattern of currents flow can also be observed at full metal plane at the bottom layer but the pattern is more dispersive than the flow of currents at the metal rings. The concentration of the currents is dependent on the operating frequency where the lowest

resonance frequency (8 GHz) is given by the largest ring while the middle resonance (10 GHz) occurs at the middle ring, and the highest resonant frequency (12 GHz) is concentrated in the smallest ring. The surface currents at the metal rings and metal plane are observed. It is shown that the anti-parallel direction of the observed excited currents proves the existence of magnetic resonance response [29]. This absorber shows high absorbance as the interaction of EM waves on the structure experiences both electric and magnetic resonances.

3. POLARIZATION SENSITIVITY AND OPERATING ANGLES

Polarization insensitive and large operating angles characteristic are the main concern in EM absorber design. These two characteristics are very important to overcoming the common limitation of absorber that operates in single polarization state and small operating angle. Perfect absorber can operate at any polarization state, having large operating angle and able to absorb almost 100% of the incident EM waves for normal incident angle. From various reports, there are a lot of metamaterial absorber designs which can absorb almost all incident EM waves for normal incident angle. But, as the incident angle is varied, the absorbance will normally decrease because the ability of the metamaterial structures to drive the circulating current in the substrate between two metallic layer is decreased [10].

As presented before, the triple band circular ring metamaterial absorber shows good absorbance for normal incident of EM waves at three resonant frequencies while the symmetrical circular geometrical property makes this structure insensitive to all polarization state for normal incident waves. To determine the response of this absorber for different angles of incident EM waves, simulation work is carried out for variation of TE and TM polarization incident waves. For TE polarization incident waves (TE mode), the electrical component of excitation EM waves is always tangential to the surface of absorber for any incident angles. For TM polarization incident waves (TM mode), the magnetic component of excitation EM waves should be tangential to the surface of absorber for all incident angles of excitation waves.

Figure 6(a) shows the simulated result of absorbance magnitudes of the proposed metamaterial absorber for TE polarization incident waves. At 0°, the absorbance at three resonant frequencies, 8 GHz, 10 GHz and 12 GHz, are 97.33%, 91.84% and 90.08%, respectively. When the incident angle is altered to 20°, the resonant frequencies are slightly shifted to higher frequency. Three corresponding resonant frequencies shifted to 8.04 GHz, 10.03 GHz and 11.79 GHz with absorbance of 99.33%, 81.01% and 93.36%, respectively. The incident angle is then altered to 40°. Thus, the corresponding resonances are observed at 8.22 GHz, 10.23 GHz and 12.03 GHz with absorbance of 99.92%, 76.46% and 75.27%, respectively. For 60°, resonant frequencies are 8.27 GHz, 10.28 GHz and 12.22 GHz with absorbance of 94.65%, 61.37% and 53.15%. It is observed that the first resonance manages to maintain high

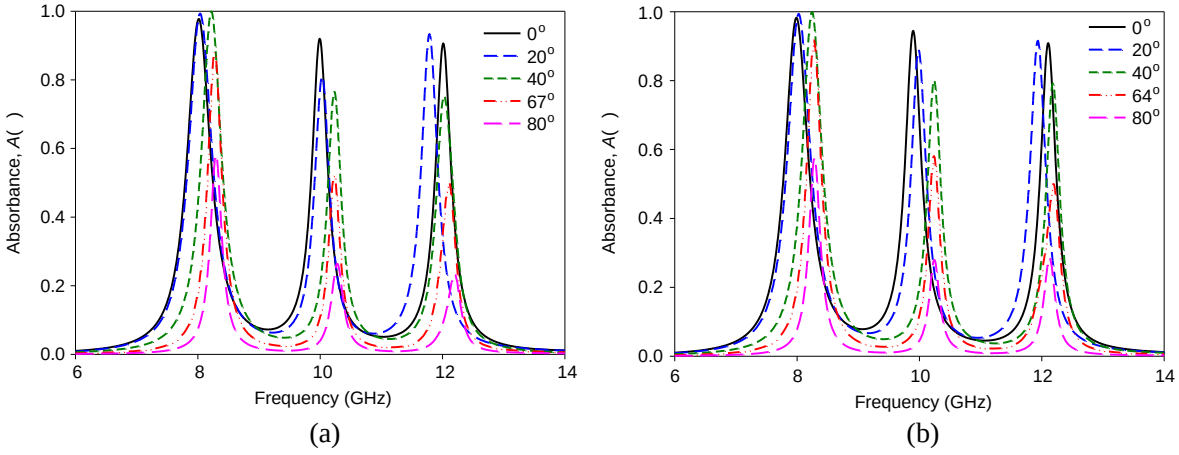

Figure 6. Absorbance for different angle of incident EM waves for (a) TE polarization and (b) TM polarization of triple band circular ring metamaterial structure.

absorbance which is above 90% for incident angle as large as 60°. The incident angle is then increased until 67°. This is found to be the maximum angle that enables the absorber to absorb at least 50% of the incident EM waves. At this incident angle, the resonant frequencies are 8.28 GHz, 10.23 GHz and 12.11 GHz with total absorbance of 88.24%, 52.34% and 50.02%, respectively. The incident angle is then extended to 80°. It is noticed that the absorbance for the first resonance is still above 50% which is 58.11% at 8.30 GHz. For the rest, 26.39% and 23.47% absorbances have been observed at 10.28 GHz and 12.20 GHz, respectively.

Figure 6(b) shows the simulated result of absorbance magnitudes of the proposed metamaterial absorber for TM polarization incident waves. At 0°, the absorbance at three resonant frequencies, 7.99 GHz, 9.90 GHz and 12.11 GHz, are 98.24%, 94.47% and 90.88%, respectively. When the incident angle is altered to 20°, the resonant frequencies are slightly shifted to higher frequency. The corresponding resonant frequencies are shifted to 8.03 GHz, 9.99 GHz and 11.94 GHz with absorbance of 99.38%, 88.93% and 91.58%. The incident angle is then altered to 40°. Thus, the corresponding resonant frequencies are shifted to 8.25 GHz, 10.24 GHz and 12.18 GHz with absorbance of 99.90%, 80.11% and 79.18%. Subsequently, the incident angle is set to 60° which generates observed resonant frequencies at 8.27 GHz, 10.22 GHz and 12.06 GHz with absorbance of 95.11%, 60.59% and 64.00%. The incident angle is then increased until 64°. This is the maximum angle that enables the absorber to absorb at least 50% of the incident EM waves. At this incident angle, the resonant frequencies are 8.28 GHz, 10.24 GHz and 12.19 GHz with absorbance of 91.66%, 58.11% and 50.00%, respectively. The incident angle is then extended to 80°. It is noticed that the absorbance for the first resonant is still above 50% which is 57.61% at 8.29 GHz. For the rest, 27.92% and 28.61% absorbances are noticed at 10.25 GHz and 12.13 GHz, respectively.

It is observed from both cases that the operating angle is nearly 65°. The incident angles larger than 65° are no longer able to drive the circulating current between two metallic layers. Hence, it causes the impedance mismatch between the metamaterial absorber and free space thus resulting in the reduction of absorbance magnitude. Overall, the results for TE and TM polarization incident waves are almost the same due to their symmetrical characteristic of circular ring.

4. FABRICATION AND MEASUREMENT

Based on the simulation, the dimension of triple circular rings metamaterial absorber is optimized. The 300 mm × 300 mm metamaterial absorber which consists of 1089 triple ring elements made of metallic copper (5.96×10^7 S/M) on FR4 dielectric substrate is fabricated using printed circuit board (PCB)

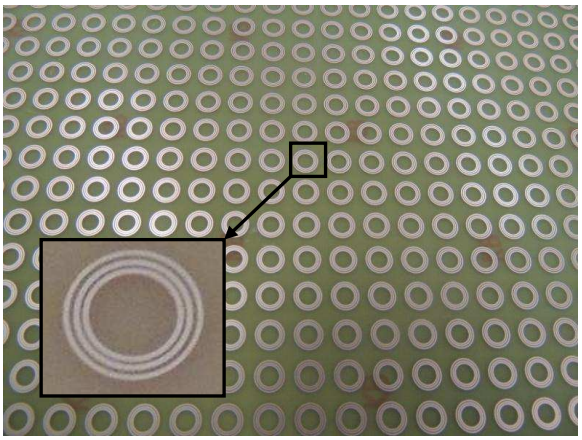

Figure 7. The fabricated triple band circular ring metamaterial absorber.

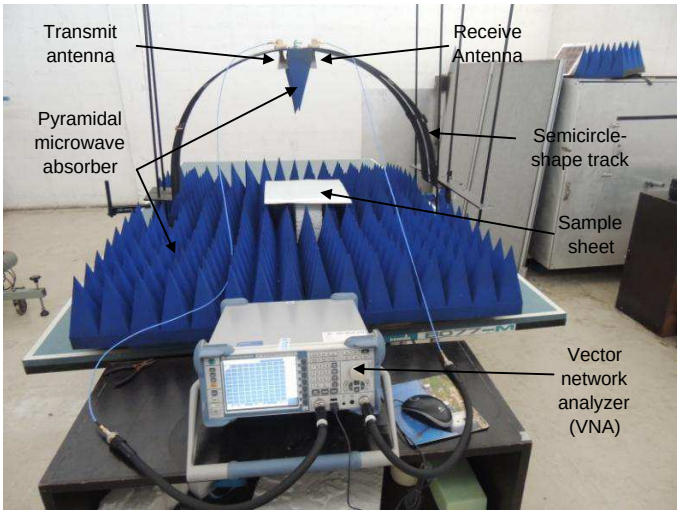

Figure 8. Measurement set-up for verifying the EM absorbing characteristic of metamaterial absorber.

technique. The structure is shown in Figure 7. The fabricated structure is then measured to verify the EM absorbing characteristics. The measurement of the metamaterial absorbing structure is carried out in a microwave anechoic chamber as shown in Figure 8. Two horn antennas are mounted on a semicircle-shaped track and can be moved to a specific angle. Both antennas are connected to a vector network analyzer (VNA) at port 1 (input) and port 2 (output). The horn antenna connected to port 1 transmits EM waves onto the sample sheet, and the reflected EM waves will be received by the horn antenna connected to port 2. The received signal presents the magnitude of reflection of the sample sheet. It will be displayed by the VNA. Pyramidal microwave absorber is placed on the surrounding of the sample sheet to eliminate any unwanted signals between the horn antennas. The reflection spectra are recorded from 7 GHz to 13 GHz by a vector network analyzer (VNA) connected to the transmitting and receiving horn antennas. In the experimental setup, reflection measurement is calibrated with an aluminum board as a perfect reflector. The sample sheet of metamaterial absorber is placed on a similar dimension of square aluminum board to measure solely on the reflection since the transmission under this arrangement is almost zero for all frequencies.

The simulated and measured EM absorbances of TE polarization incident waves for normal incident waves are compared and shown in Figure 9. The experimental result is comparable to the simulated one with a slight frequency shift. The simulated absorbance at three resonance frequencies, 8 GHz, 10 GHz and 12 GHz, are 97.33%, 91.84% and 90.08%, respectively. In measurement, the corresponding resonant frequencies shift to 8.10 GHz, 10.14 GHz and 12.14 GHz with the absorbance of 91.88%, 83.11% and 85.74%, respectively. The absorbance values from measurement are slightly lower than the simulation. This can be due to the scattering from the structure and the mutual coupling between both horn antennas [1]. The frequency shift occurs due to the fabrication tolerance and dielectric dispersion of the substrate. The FWHM from simulation are 3.69%, 2.90% and 3.36% at 8 GHz, 10 GHz and 12 GHz, respectively. For measurement, FWHM are 3.27%, 2.77% and 4.16% at 8.10 GHz, 10.14 GHz and 12.15 GHz, respectively. The FWHM results for the measurement are well agreed with the simulation.

Figure 10 shows the measured result of triple band circular ring metamaterial absorber for TE and TM polarization incident waves. The measurement is done for oblique incident angle of 0°, 20°, 40°, and 60°. Incident angle larger than 60° cannot be carried out due to the effect of direct coupling between the transmit and receive antennas. For better measurement result, highly directive transmitted and received antennas can be used with small side lobes.

Figure 10(a) shows the measured result of absorbance magnitudes of triple band circular ring metamaterial absorber for TE polarization incident waves. It shows that the operating frequencies for all cases are slightly shifted to higher frequency due to the same reason as mentioned previously. At 0° incidence angle, the absorbance at three resonance frequencies, 8.10 GHz, 10.14 GHz and 12.14 GHz, are 91.88%, 83.11% and 85.74%, respectively. When the incident angle is altered to 20°, the resonant frequencies are 8.10 GHz, 10.15 GHz and 12.15 GHz with absorbance of 85.21%, 86.03% and 76.54%,

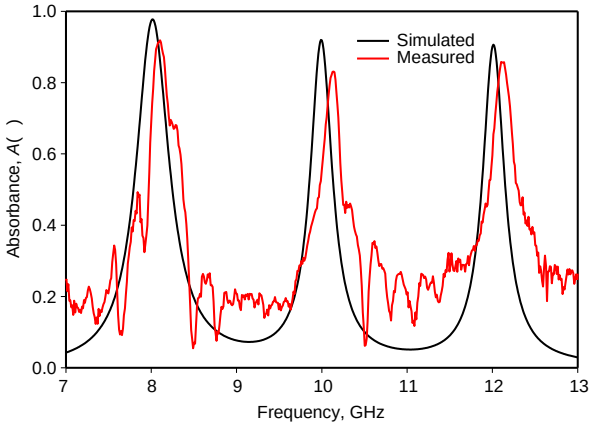

Figure 9. Simulated and measured EM absorbance for triple band circular ring metamaterial absorber at normal incident angle.

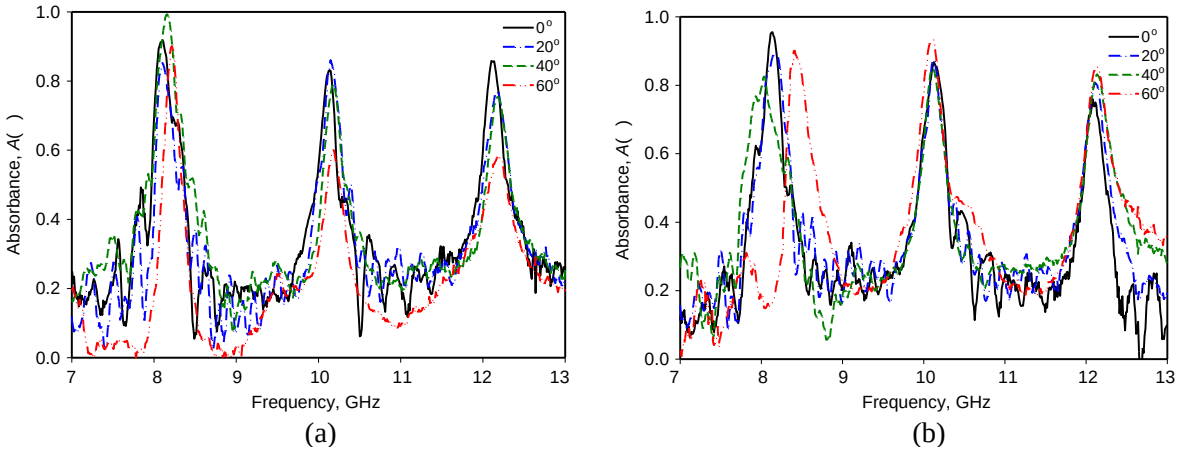

Figure 10. Measured result of absorbance for different angle of incident EM waves for (a) TE polarization and (b) TM polarization of triple band circular ring metamaterial structure.

respectively. The incident angle is then altered to 40°. The measured resonance frequencies are shifted to 8.16 GHz, 10.18 GHz and 12.18 GHz with absorbance of 99.29%, 79.14% and 75.42%. Next, the absorbance is observed for incident angle of 60°. The measured resonant frequencies are 8.21 GHz, 10.18 GHz and 12.18 GHz with the absorbance of 90.09%, 60.04% and 58.67%, respectively.

Figure 10(b) shows the measured result of absorbance magnitudes of triple-band circular ring metamaterial absorber for TM polarization incident waves. At 0°, the absorbance at three resonance frequencies, 8.14 GHz, 10.13 GHz and 12.08 GHz, are 95.54%, 86.75% and 75.98%. When the incident angle is altered to 20°, the resonant frequencies are 8.16 GHz, 10.11 GHz and 12.11 GHz with absorbance of 89.76%, 87.56% and 80.69%, respectively. The incident angle is then altered to 40°. The resonant frequencies are shifted to 8.03 GHz, 10.10 GHz and 12.14 GHz with absorbance of 82.56%, 85.00% and 83.21%. The incident angle is then increased to 60°. The resonance frequencies are 8.41 GHz, 10.10 GHz and 12.13 GHz with the absorbance of 90.11%, 93.42% and 85.67%, respectively.

From the measurement result, it is observed that the difference of oblique incident EM waves gives a slight effect on the resonant frequencies. However, the absorbance magnitudes from measurement are higher than the simulation for large oblique incident angles. This is due to the direct coupling between the transmitted and received horn antennas. It is suggested that the measurement should be done in larger anechoic chamber room and using the integration of electromagnetic lens with the transmitted and received horn antennas to focus the beam of the antennas so that it can be more directive. Overall, the resonant behavior of the triple-band circular ring metamaterial absorber is successfully observed for the three resonant frequency of interest.

5. CONCLUSION

In summary, a triple-band circular ring metamaterial absorber has been designed, fabricated and measured. The performance of this metamaterial absorber is observed in term of absorbance and operating angle. The measured and simulated results agree well with each other with slight frequency shift. To understand the physical behavior of the triple-band circular metamaterial absorber, the surface current, electric field and magnetic field distribution are plotted and studied. For future work, several structures will be studied which can work at multi-band frequencies with high absorbance that can maintain at least 95% of absorbance up to 40° incident electromagnetic waves.

ACKNOWLEDGMENT

The authors thank the Ministry of Higher Education (MOHE) for supporting the research work, Research Management Centre (RMC), School of Postgraduate (SPS), Communication Engineering

Department (COMM) Universiti Teknologi Malaysia (UTM) and all members of Advanced Microwave Lab P18 FKE-UTM for giving motivation, knowledge sharing and support of the research under grant No. R.J130000.7923.4S007/04H38/4L811.

REFERENCES

1. Gangwar, A. and S. C. Gupta, "Metamaterials — A new era of artificial materials with extraordinary properties," *International Journal of Engineering Research and Management Technology*, Vol. 1, No. 2, 76–84, 2014.
2. Chen, H. S., L. Huang, X. X. Cheng, and H. Wang, "Magnetic properties of metamaterial composed of closed rings," *Progress In Electromagnetics Research*, Vol. 115, 317–326, 2011.
3. Han, N. R., Z. C. Chen, C. S. Lim, B. Ng, and M. H. Hong, "Broadband multi-layer terahertz metamaterials fabrication and characterization on flexible substrates," *Optics Express*, Vol. 19, No. 8, 6990–6998, 2011.
4. Kim, D.-S., D.-H. Kim, S. Hwang, and J.-H. Jang, "Broadband terahertz absorber realized by self assembled multi-layer glass spheres," *Optics Express*, Vol. 20, No. 12, 13566–13572, 2012.
5. Majid, H. A., M. K. A. Rahim, and T. Masri, "Left-handed metamaterial design for microstrip antenna application," *2008 IEEE International RF and Microwave Conference Proceeding*, 218–221, 2008.
6. Garg, B. and D. Saleem, "Experimental verification of double negative property of LHM with significant improvement in microstrip transceiver parameters in S band" *International Journal of Engineering Practical Research (IJEPR)*, Vol. 2, No. 2, 64–70, 2013.
7. Zarifi, D., S. E. Hosseininejad, and A. Abdolali, "Design of dual-band double negative metamaterials," *Iranian Journal of Electrical & Electronic Engineering*, Vol. 10, No. 2, 75–80, 2014.
8. Shi, Y. and C.-H. Liang, "The analysis of double-negative materials using multi-domain pseudospectral time-domain algorithm," *Progress In Electromagnetics Research*, Vol. 51, 153–165, 2005.
9. Schurig, D., J. J. Mock, B. J. Justice, S. A. Cummer, J. B. Pendry, A. F. Starr, and D. R. Smith, "Metamaterial electromagnetic cloak at microwave frequencies," *Science*, Vol. 314, 977–980, 2006.
10. Huang, Y., G. wen, and W. Zhu, "Experimental demonstration of a magnetically tunable ferrite based metamaterial absorber," *Optics Express*, Vol. 22, No. 13, 16408–16417, 2014.
11. Liu, X. L., L. P. Wang, and Z. M. Zhang, "Wideband tunable omnidirectional infrared based on doped-silicon nanowire arrays," *Journal of Heat Transfer*, Vol. 135, No. 6, 061602, 2013.
12. Chang, Y. C., C. M. Wang, M. N. Abbas, M. H. Shih, and D. P. Tsai, "T-shaped plasmonic array as a narrow band thermal emitter or biosensor," *Optics Express*, Vol. 17, No. 16, 13526–13531, 2009.
13. Zhao, J., Y. Feng, B. Zhu, and T. Jiang, "Sub-wavelength image manipulating through compensated anisotropic metamaterial prisms," *Optics Express*, Vol. 16, No. 22, 18057–18066, 2008.
14. Che Seman, F. and R. Cahill, "Frequency selective surfaces based planar microwave absorbers," *PIERS Proceedings*, 906–909, Kuala Lumpur, Malaysia, Mar. 27–30, 2012.
15. Huang, L. and H. Chen, "Multi-band and polarization insensitive metamaterial absorber," *Progress In Electromagnetics Research*, Vol. 113, 103–110, 2011.
16. Li, M.-H., H.-L. Yang, and X.-W. Hou, "Perfect metamaterial absorber with dual bands," *Progress In Electromagnetics Research*, Vol. 108, 37–49, 2010.
17. Wang, J. F., S. B. Qu, Z. T. Fu, H. Ma, Y. M. Yang, and X. Wu, "Three-dimensional metamaterial microwave absorbers composed of coplanar magnetic and electric resonators," *Progress In Electromagnetics Research*, Vol. 7, 15–24, 2009.

18. Park, J. W., P. V. Tuong, J. Y. Rhee, K. W. Kim, W. H. Jang, E. G. Choi, L. Y. Chen, and Y. P. Lee, "Multi-band metamaterial absorber based on the arrangement of donut-type resonators," *Optics Express*, Vol. 21, No. 8, 9691–9702, 2013.
19. Cheng, Y., Y. Nie, and R. Gong, "Design of a wide-band metamaterial absorber based on fractal frequency selective surface and resistive films," *Phys. Scr.*, Vol. 88, 045703, 2013.
20. Landy, N. I., S. Sajuyigbe, J. J. Mock, D. R. Smith, and W. J. Padilla, "Perfect metamaterial absorber," *Physical Review Letters*, Vol. 100, 207402, 2008.
21. Dincer, F., O. Akgol, M. Karaaslan, E. Unal, and C. Sabah, "Polarization independent perfect metamaterial absorbers for solar cell application in the microwaves, infrared, and visible regime," *Journal of Electromagnetic Waves and Applications*, Vol. 23, No. 7, 953–962, 2009.
22. Tao, H., N. I. Landy, C. M. Bingham, X. Zhang, R. D. Averitt, and W. J. Padilla, "A metamaterial absorber for the terahertz regime: Design, fabrication and characterization," *Optics Express*, Vol. 16, 7181–7188, 2008.
23. Wang, J. Q., C. Z. Fan, P. Ding, J. N. He, Y. G. Cheng, W. Q. Hu, G. W. Cai, E. J. Liang, and Q. Z. Xue, "Tunable broad-band perfect absorber by exciting of multiple plasmon resonances at optical frequency," *Optics Express*, Vol. 20, 14871–14878, 2012.
24. Tao, H., C. M. Bingham, A. C. Strikwerda, D. Pilon, D. Shrekehamer, N. I. Landy, K. Fan, X. Zhang, W. J. Padilla, and R. D. Averitt, "Highly flexible wide angle incidence terahertz metamaterial absorber: Design, fabrication and characterization," *Phys. Rev. B*, Vol. 78, No. 7, 241103, 2008.
25. Dincer, F., M. Karaaslan, E. Unal, K. Delihacioglu, and C. Sabah, "Design of polarization and incident angle insensitive dual-band metamaterial absorber based on isotropic resonators," *Progress In Electromagnetics Research*, Vol. 144, 123–132, 2014.
26. Sabah, C., F. Dincer, M. Karaaslan, E. Unal, and O. Akgol, "Polarization-insensitive FSS based perfect metamaterial absorbers in GHz and THz frequencies," *Radio Science*, Vol. 49, 306–314, 2014.
27. Huang, L. and H. Chen, "Multi-band and polarization insensitive metamaterial absorber," *Progress In Electromagnetics Research*, Vol. 113, 103–110, 2011.
28. Sun, J., L. Liu, G. Dong, and J. Zhou, "An extremely broad band metamaterial absorber based on destructive interference," *Optics Express*, Vol. 19, No. 22, 21155–21162, 2011.
29. Tao, H., N. I. Landy, C. M. Bingham, X. Zhang, R. D. Averitt, and W. J. Padilla, "A metamaterial absorber for the terahertz regime: Design, fabrication and characterization," *Optics Express*, Vol. 16, No. 10, 7181–7188, 2008.